Surface plasmon wave propagation along single metal wire*

Zhong Ren-Bin(钟任斌), Liu Wei-Hao(刘维浩), Zhou Jun(周 俊), and Liu Sheng-Gang(刘盛纲)†

Terahertz Science and Technology Research Centre, University of Electronic Science and Technology of China, Chengdu 610054, *China*

(Received 23 February 2012; revised manuscript received 2 May 2012)

Recently, the single metal wire (SW) has become attractive for its potential applications in the terahertz and higher frequency range. However, as the most simple and typical surface plasmon polariton (SPP) transmission line, its study seems far from enough. Many important transmission behaviours have not been explained satisfactorily from the viewpoint of physics. In this paper, making use of the modified Drude model (MDM) based on the Sommerfeld theory, the transmission behaviours of SPPs along SW are systemically investigated theoretically. Some important physical phenomena such as the mode transformation, the lifetime of the radiative mode and the resonance frequency are revealed, and their mechanisms are explored. The results obtained in the paper will facilitate a general understanding of the features and the physical essence of the SPP transmission, not only for SW itself but also for other SPP transmission lines.

Keywords: surface plasmon, single metal wire, wave propagation

PACS: 73.20.Mf, 84.40.Az, 71.36.+c **DOI:** 10.1088/1674-1056/21/11/117303

1. Introduction

Recently, the single metal wire (SW) has aroused great interest, owing to its advantages of low loss and low dispersion in transmitting electromagnetic (EM) waves from the terahertz to light regime via surface plasmon polaritons (SPPs).[1−9]

As a simplest and typical SPP transmission line, so many research studies on SW were conducted for the axial symmetric mode (TM_0 mode).[1−3] In Ref. [4], were gave out some important transmission features of the axial asymmetric modes on SW, showing that besides the surface waves (real modes), there are also radiation waves (virtual modes) for the asymmetric mode. The behaviour of the negative dispersion and cutoff frequency are presented. However, no satisfactory physical explanation on these phenomena has been given till now.

Some problems on the SW transmission features still need to be further explored. For example, what will happen when the field penetration into the wire becomes very strong for a very thin wire? Will an excited mode at import of the SW be transformed into another mode, and what is the physical mechanism for such a mode transformation? How is the lifetime of the mode estimated? What is the mechanism for the occurrence of the radiative SPP mode on SW? How are the resonance (asymptotic) frequency and the cutoff frequency determined? The above problems show the necessity and urgency in performing a further systematical investigation on the SPP transmission along the SW.

In addition, in previously published papers,[1−6] the Drude Model (DM) [10] or even the simplified DM was used to describe the dielectric characteristics of the metal. However the DM is actually an approximate model that is based on the assumption that the ideal free electron gas in the metal has a Maxwell–Boltzmann distribution. Therefore, it is not so accurate for real metals.[11] Fortunately, decades later, with the help of the quantum theory, the modified Drude model (MDM) came into being based on the Sommerfeld theory of metal. In the MDM, the Maxwell–Boltzmann distribution in DM is replaced by the Femi–Dirac distribution.[12] According to the MDM, the interaction of free electrons with the EM field can be treated with classical theory under the following two limitations: the energy gained by the

*Project supported by the Specialized Research Fund for Doctoral Program of Higher Education of China (Grant No. 20100185110022), the National Basic Research Program of China (Grant No. 2007CB310401), and the Fundamental Research Funds for the Central Universities of Ministry of Education of China (Grant No. ZYGX2011J037).

†Corresponding author. E-mail: liusg@uestc.edu.cn

© 2012 Chinese Physical Society and IOP Publishing Ltd

free electrons from the incident fields cannot exceed the threshold of the quantum transition of electrons in the metal (Ag: 2.7 eV, Au: 1.4 eV); the absorbed energy cannot exceed the work function of the electrons to avoid them escaping from the metal.

In this paper, the MDM with data of the experimental measurements taken into consideration is adopted to express the dielectric function of the real metal.[13] The transmission and radiation characteristics of the SPPs along SW are investigated in detail. We focus on the exploration of the physical explanation and mechanism of the transmission behaviours of SW, and some important physical phenomena are revealed for the first time.

The rest of the paper is organized as follows. In Section 2 we show the calculated dispersion behaviours of the SPPs propagating along a SW based on the MDM, some important and interesting phenomena are presented here. The results of the computer simulation are given in Section 3. The physical mechanism of the phenomenon presented in Section 2 is given in Section 4. Some conclusions are drawn from this study in Section 5.

2. Behaviours of SPP propagation along SW

The physical model considered in this paper is a nonmagnetic SW in the air with a radius of $a = D/2$, where D is the diameter of SW. The Maxwell equations are solved in a cylindrical coordinate system with continuous boundary conditions on the cylinder surface (the tangential components of the electric field and the magnetic field must be continuous at the wire surface $r = a$), we can obtain the dispersion equation of the electromagnetic wave propagation in the z direction along the wire as[4,14]

$$\left(\frac{1}{k_{\rm ci}a}\frac{{\rm J}'_{\rm m}(k_{\rm ci}a)}{{\rm J}_{\rm m}(k_{\rm ci}a)} - \frac{1}{k_{\rm co}a}\frac{{\rm H}^{(1)'}_{\rm m}(k_{\rm co}a)}{{\rm H}^{(1)}_{\rm m}(k_{\rm co}a)}\right) \times \left(\frac{k^2_{0i}}{k_{\rm ci}a}\frac{{\rm J}'_{\rm m}(k_{\rm ci}a)}{{\rm J}_{\rm m}(k_{\rm ci}a)} - \frac{k^2_{0o}}{k_{\rm co}a}\frac{{\rm H}^{(1)'}_{\rm m}(k_{\rm co}a)}{{\rm H}^{(1)}_{\rm m}(k_{\rm co}a)}\right) = m^2k_z^2\left(\frac{1}{(k_{\rm co}a)^2} - \frac{1}{(k_{\rm ci}a)^2}\right)^2. \quad (1)$$

Here, $\rm J_m$ and $\rm H^{(1)}_m$ are the fist kind of Bessel function and the Hankel function respectively, $k^2_{\rm ci} = k_0^2\varepsilon_{\rm m} - k_z^2$, $k^2_{\rm co} = k_0^2\varepsilon_{\rm a} - k_z^2$, with $\varepsilon_{\rm m}$ and $\varepsilon_{\rm a}$ being the permittivities of the metal and air respectively. In Eq. (1), the TE and TM modes are coupled with each other except the axial symmetric modes ($m = 0$); it can be simplified as

$$\frac{1}{k_{\rm ci}a}\frac{{\rm J}'_{\rm m}(k_{\rm ci}a)}{{\rm J}_{\rm m}(k_{\rm ci}a)} - \frac{1}{k_{\rm co}a}\frac{{\rm H}^{(1)'}_{\rm m}(k_{\rm co}a)}{{\rm H}^{(1)}_{\rm m}(k_{\rm co}a)} = 0 \quad (2)$$

for $\rm TM_0$ mode;

$$\frac{k^2_{0i}}{\mu_i k_{\rm ci}a}\frac{{\rm J}'_{\rm m}(k_{\rm ci}a)}{{\rm J}_{\rm m}(k_{\rm ci}a)} - \frac{k^2_{0o}}{\mu_o k_{\rm co}a}\frac{{\rm H}^{(1)'}_{\rm m}(k_{\rm co}a)}{{\rm H}^{(1)}_{\rm m}(k_{\rm co}a)} = 0 \quad (3)$$

for $\rm TE_0$mode.

Making use of the MDM, the dielectric characteristic of the real metal is

$$\varepsilon_{\rm m} = \varepsilon_\infty - \frac{\omega_{\rm p}^2}{\omega^2 + {\rm j}\,\gamma\omega}, \quad (4)$$

where $\omega_{\rm p}$ is the plasma frequency of the metal, γ is the mean collision frequency of electrons. The value of ε_∞ is in the range of 1–10, depending on the metal type.[11,12] For silver wire, the parameters are $\omega_{\rm p} = 1.39 \times 10^{16}$, $\gamma = 3.2 \times 10^{13}$, and $\varepsilon_\infty = 4.5$ obtained by fitting the experimental data in Ref. [13].

Based on Eqs. (1)–(4), the dispersion curves of the SPPs propagating along the silver wire with diameters of 440 nm, 44 nm, and 4.4 nm are obtained; the results are shown respectively in Figs. 1–3, where the right and the left region of the light line are the slow wave region (real modes, surface waves) and the fast waves region (virtual modes, radiation waves), respectively. Figure 1 shows the comparisons between the dispersion curves obtained by the MDM and those by the DM as given in Ref. [4] for different modes of the waves and different diameters of the wires. We can see that the curves derived by both models are similar, but for the former ones, the highest frequencies decrease and the frequency bands are narrower. The differences are due to the decrease of the surface plasmon resonance frequency ($\omega_{\rm s}$), which will be discussed later in the paper.

Further investigations on these results show the following interesting and important transmission behaviours of SW.

1) For the axial symmetric mode ($\rm TM_0$ mode) as shown in Fig. 2(a), the dispersion curves are always on the right side of the light line (slow wave region), indicating that the $\rm TM_0$ mode is a surface wave with velocity less than the speed of light. This result is in accordance with the results presented in Refs. [1]–[3]. The simulated field pattern at 900 THz for the $\rm TM_0$ mode on silver SW is shown in Fig. 2(b), which indicates that the axial symmetric fields concentrate mainly in the vicinity of the surface of the wire. The three-dimensional (3D) simulation in Fig. 2(c) shows the stable propagation of $\rm TM_0$ mode.

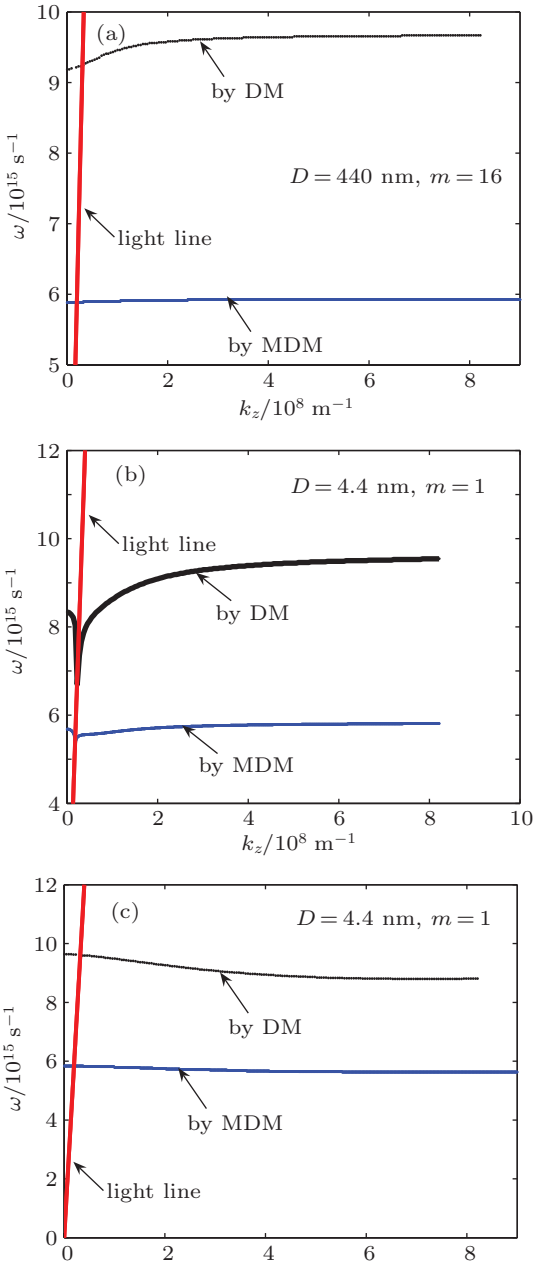


Fig. 1. (colour online) Comparison between the dispersion relation of silver SW obtained by MDM and that obtained by MD in Ref. [4] with (a) $D = 440$ nm, $m = 16$; (b) $D = 44$ nm, $m = 1$; (c) $D = 4.4$nm, $m = 1$.

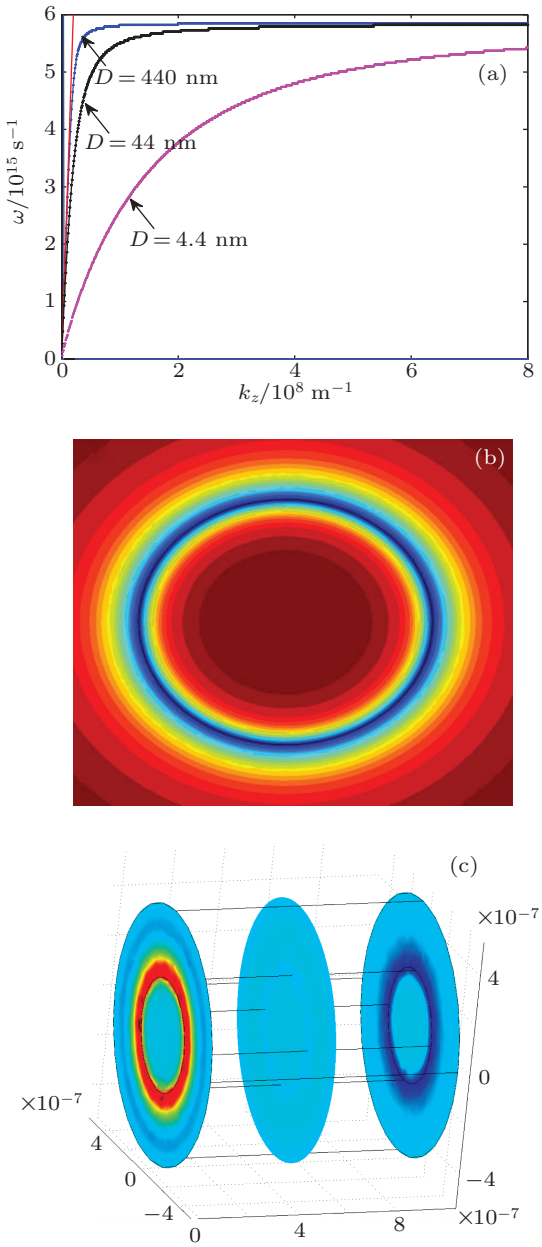


Fig. 2. (colour online) (a) Dispersion curves of TM_0 mode for different diameters of 440 nm, 44 nm, and 4.4 nm; (b) simulated field distribution on the cross section of 440 nm silver wire; (c) stable transmission of TM_0 mode on 440 nm silver wire, obtained by 3D simulation.

2) For the asymmetric mode, the dispersion features shown in Fig. 3 are quite different from those of the symmetric mode. Firstly, the dispersion curves traverse the light line and are located in the slow wave region as well as the fast wave region, which means that both the transmission wave and radiation wave appear in this case. Secondly, the radiation waves have cutoff frequencies, whose values depend on the mode number of the wave and the diameter of the wire. Thirdly, the dispersion curves become flat and squeeze together with the increase of the mode number or the decrease of the diameter, which indicates that the thick wire can sustain more propagation modes than the thin wire. Finally, the negative dispersion behaviour can be found for the thin wire as shown in Figs. 3(b) and 3(c), but for the thick wire, the dispersion curves in Fig. 3(a) are positive for the mode numbers 1–16.

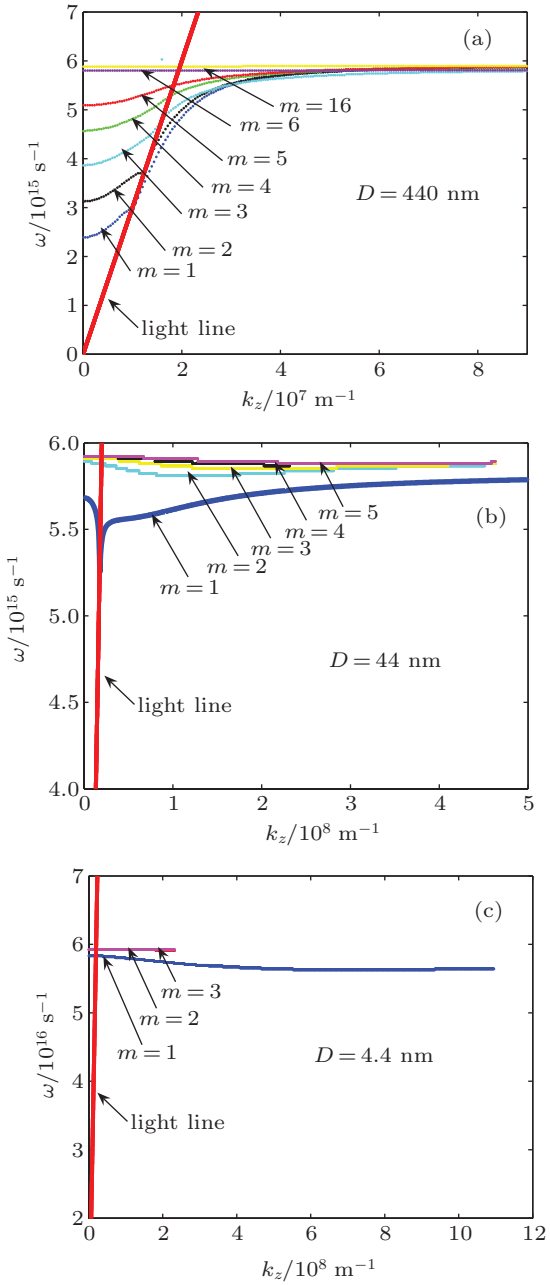


Fig. 3. (colour online) Dispersion curves for different modes with diameters of (a) 440 nm, (b) 44 nm, (c) 4.4 nm of silver SW.

Some of the phenomena presented above have been found in previous studies,[4,15,16] but it seems that more reasonable explanations and more knowledge of the mechanisms of the occurrence of these phenomena need to be explored for a deeper understanding of the SPP transmission features along SW, and this is what we try to do in the following sections.

3. Computer simulations on asymmetric modes

From the dispersion behaviours of the SPPs on SW shown in the previous section, we can see that the dispersion characteristics of the asymmetric modes strongly depend on the ratio of the diameter of the wire (D) to the wavelength (λ) of the transmission wave. In order to see the influence of the dimension of the wire on its transmission features more clearly, computer simulations on the asymmetric modes are performed using commercial finite element software COMSOL Multiphysics. The field patterns on the cross section of the silver wire with diameters of 440 nm and 4.4 nm for different modes are shown in Fig. 4, we can see that the field distributions vary azimuthally according to the mode number for all asymmetric modes, but for the same modes they are significantly different from each other for different diameters. At 900 THz ($\lambda = 330$ nm), for thick wire ($D = 440$ nm) as shown in Fig. 4(a), both the penetration depth of the wave fields into the metal and the decay length of the field into the air are very small compared with the diameter of the wire, and the fields concentrate only in the vicinity of the surface of the metal wire; but for very thin wire with $D \ll \lambda$ ($D = 4.40$ nm) as shown in Fig. 4(b), the penetrated fields fill almost the whole space within the wire. So, the field penetration into the wire strongly depends on the ratio of the diameter to the wavelength, and the strength of the penetrated field increases as the diameter of the wire decreases.

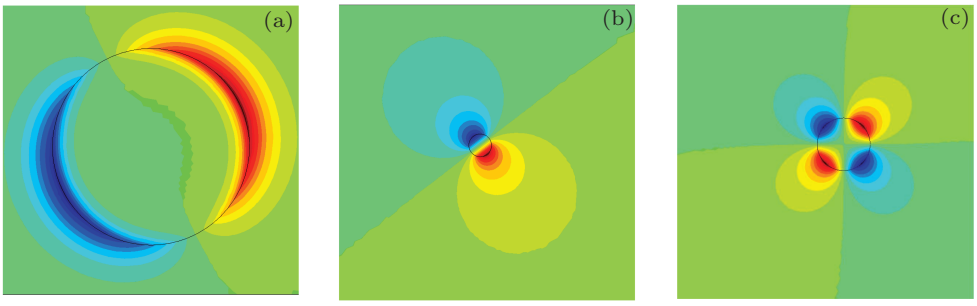


Fig. 4. (colour online) Field patterns on the cross section for silver wire at 900 THz: (a) 440 nm diameter with mode $m = 1$, and 4.4 nm diameter with (b) mode $m = 1$ and (c) with mode $m = 2$.

Another interesting phenomenon found by our simulations is the mode transformation for the very thin wire ($D = 4.4$ nm). As shown in Fig. 5(a), the excited asymmetric mode ($m = 2$) at the import of the wire radiates off very quickly, shortly after that, the symmetric mode ($m = 0$) takes it over and propagates along the wire steadily, and Fig. 5(b) implies that this process happens in a very short time. While for the thick wire case ($D = 440$ nm), the excited asymmetric mode can directly go into a stable propagation along the wire as shown in Fig. 6. It means that when the diameter of the wire is much less than the wavelength, SW cannot effectively transmit asymmetric modes any more, mode transformation happens, and the asymmetric mode with $m = 2$ is transformed into a symmetric mode with $m = 0$. It is the first time the mode transformation in the SW has been revealed. The mechanism for the appearance of this interesting and important phenomenon will be given in the next section.

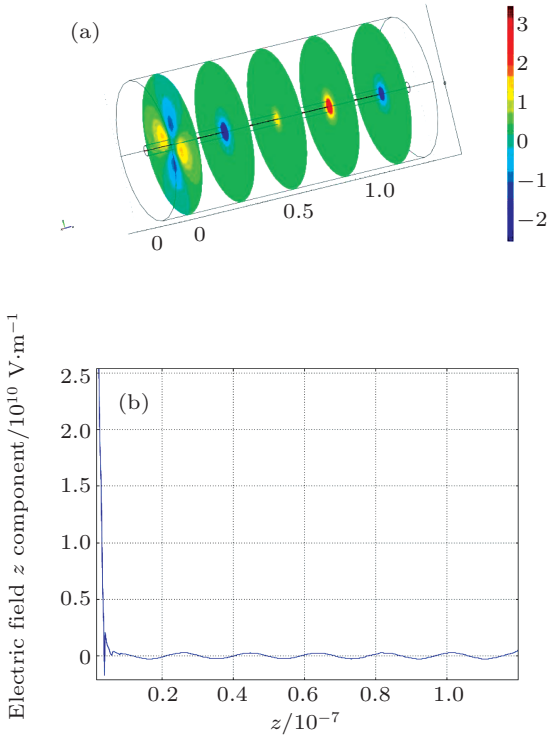


Fig. 5. (colour online) (a) Transformation process from $m = 2$ asymmetric mode to TM_0 mode and (b) the fields along the very thin silver wire with a diameter of 4.4 nm.

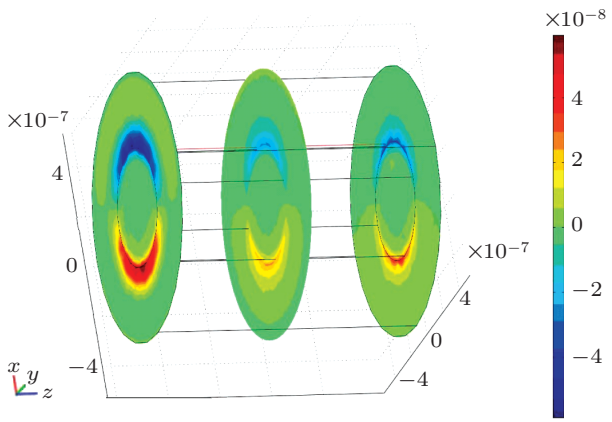


Fig. 6. (colour online) Stable transmission of $m = 1$ asymmetric mode along the silver wire with a diameter of 440 nm.

4. Physical mechanisms

In this section, we will discuss the physical explanation for the phenomena presented in Sections 2 and 3, and the mechanisms of some newly revealed phenomena, such as mode transformation, will be explored from the viewpoint of physics.

Owing to the fact that the MDM is based on the Sommerfeld theory of metal, Maxwell's equations and Newton's theory can be used to deal with the interaction between the free electrons in the metal and the penetrated EM fields: under the excitations of the penetrated fields, the free electrons will execute a collective motion. For an SW, in particular a thin SW, subjected to the penetrated fields, the uniformly distributed free electrons within the wire are re-arranged to form a bunch-like state. On the other hand, due to the space charge effect, the electrons tend to return to their original uniform spatial distribution. These processes are the general physical basis of the following analyses.

4.1. Radiation of asymmetric modes

When the TM_0 mode is excited (symmetric excitation) on the SW, the free electrons in the metal can oscillate longitudinally only in the vicinity of the surface of the wire, which is just the case of SPPs. So, the TM_0 mode is always the surface propagating mode as shown in Fig. 2. Yet, when the wire is excited by an asymmetric mode (asymmetric excitation) as shown in Fig. 7, the natural uniformly distributed free electrons in the metal are forced to change into electron bunches along the angular direction within the wire to match the azimuthal variation of the penetrated fields; the electron bunches will execute spiral motion along the wire by combining the longitudinal and transversal motions of the electrons. According to the electrodynamics theory, the transversal rotation of the electron bunches will emit EM radiation, which is just the physical mechanism of the radiation of the asymmetric mode.

The formulas for the calculation of the radiation power can be found in Appendix A.

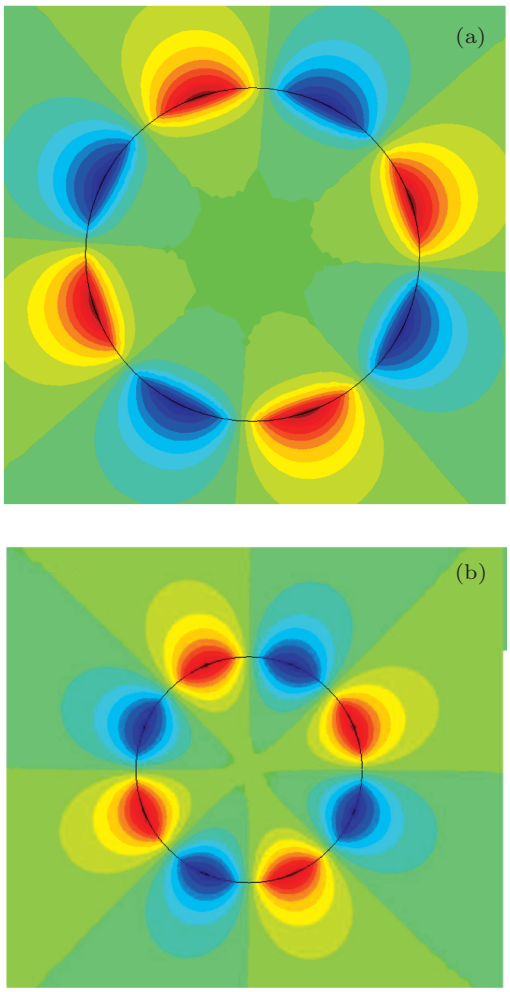


Fig. 7. (colour online) Field patterns of $m = 4$ asymmetric mode on the cross section of the silver wire with diameters of (a) $D = 440$ nm, (b) $D = 44$ nm.

4.2. Mode transformation and lifetime

Now, the mechanism of the mode transformation for SPPs propagating along SW can be explored. When an asymmetric mode is excited on a very thin metal wire, the field penetration into the wire is very strong as shown in Figs. 4(b) and 4(c); the free electrons are forced to change their original uniform spatial distribution state, and the distribution re-arrangement of free electrons occurs in the wire to form electron bunches, which will also execute a special spiral motion along the wire. This motion causes the asymmetric mode to rapidly disappear through radiation. On the other hand, the variation of the spatial distribution of the electrons will result in a strong space charge force, which leads to a reverse trend for the re-arranged electron distribution returning to the original uniform state gradually. This process gives birth to the symmetric mode (TM_0 modes) for a subsequent stable propagation: the mode transformation is completed. The mode transformation is a transient process, which takes a very short time on the order of attosecond according to the simulation shown in Fig. 5(b), and this time is just the lifetime of the radiated asymmetric mode, which is reasonable compared with the relaxation time of the electrons in the metal.[12]

4.3. Resonance (asymptotic) frequency and cutoff frequency

As shown in Fig. 3, the dispersion curves for all modes on SW will finally approach to resonance (asymptotic) frequency ω_s. Similar to that for planar structure, ω_s is also very important for describing the features of the dispersion behaviours of the SPPs along the cylindrical wire.

For SPPs on planar structure, the dispersion equation is simple and can be expressed as[17]

$$k_z = \frac{\omega}{c}\sqrt{\frac{\varepsilon_d \varepsilon_m}{\varepsilon_d + \varepsilon_m}}. \tag{5}$$

The resonance will occur for very large k_z, and we can obtain $\varepsilon_d + \varepsilon_m \to 0$ from Eq. (5), then there is

$$\omega_s = \frac{\omega_p}{\sqrt{\varepsilon_\infty + \varepsilon_d}}. \tag{6}$$

Here, we treat the problem from the viewpoint of physics. As is well known, the group velocity represents the transmission of energy or signal of the EM wave, it is defined as

$$v_g = \left(\frac{\partial k_z}{\partial \omega}\right)^{-1}. \tag{7}$$

As the group velocity approaches to zero ($v_g \to 0$), the energy transmission along the wire will stop and the resonance happens. So, by substituting Eq. (5) into Eq. (7) and letting $v_g \to 0$, we can also obtain the resonant frequency of the SPPs in the planar interface as shown in Eq. (6).

This treatment is also valid for a cylindrical structure, for which the dispersion relation as shown in Eq.(1) is much more complicated, so the analytical derivation of ω_s seems hard. Instead, the numerical calculation can be carried out and the results are given in Appendix B. It shows clearly that ω approaches to ω_s when $(\partial k_z/\partial\omega)^{-1} = 0$, where $k_z$exhibits a large value. The following important points should be noticed for the ω_s of the SPPs:

(1) the values of ω_s are the same for planar and cylindrical structures, so ω_s is one of the general parameter of SPPs;

(2) for a cylindrical structure, the value of ω_s is independent of the diameter of the wire;

(3) the diameter of the wire influences only the speed of ω approaching to ω_s: the thinner the wire, the slower the speed approaching to ω_s is.

The cutoff frequency of the SW can be calculated by the dispersion equations (1)–(3) with $k_z = 0$. The dependence of the cutoff frequency of the asymmetric modes on the azimuthal mode number are shown by Fig. 8 for the silver wire with diameters of 4.4, 44, and 440 nm. We can see that the cutoff frequencies increase with the mode number increasing, but they are always less than ω_s.

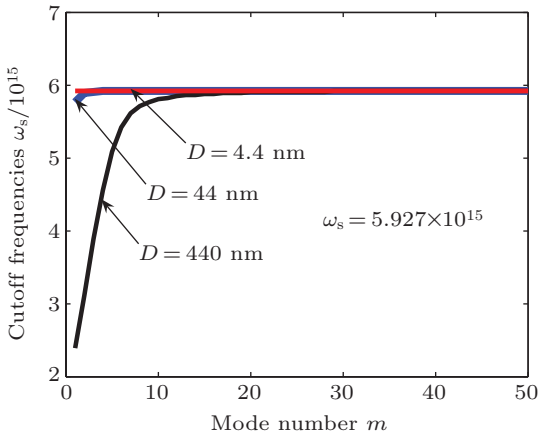


Fig. 8. (colour online) Variations of cutoff frequencies of silver SW with mode number for wires with different diameters.

The cutoff frequencies come from the predominant azimuthal propagation of the SPPs on the SW, which is perpendicular to the longitudinal direction, just similar to the transversal propagating of SPPs on planar structure. When the azimuthal component of the SPP propagation becomes overwhelming compared with the longitudinal component, the cutoff frequency occurs. The cutoff frequency of the SW is different from that of the closed waveguide. For example, for hollow rectangular and cylindrical waveguides their cutoff frequencies depend on the transverse resonance in the closed waveguide. As is well known, there exists a relationship $\lambda_c = 2b$ for the TM_0 mode in a rectangular waveguide. However, for the open SW system, the wavelength shortening phenomenon appears in the angular direction both inside and outside of the wire, there exists a relationship $(\lambda_c)_{EH_1} < \pi d$.

4.4. Negative dispersion

As mentioned above, when the asymmetric modes are excited in the wire, the bulk free electrons in the metal will be forced to form electron bunches along the azimuthal direction of the wire. These bunches will interact with each other in the transversal direction and the interactions become considerable when the wire is very thin. These strong interactions cause the electron bunches to vibrate strongly in the transversal direction. When the transversal vibration, instead of the longitudinal motion, becomes the dominant motion of the free electrons in the metal, the negative dispersion occurs just like that in the case of the planar thin film.[17]

5. Conclusions

Making use of the MDM, the systematical investigation by means of analytical theory and computer simulations on the SPP transmission along the SW are implemented in depth in this paper. The following results are obtained.

(i) For the SPP propagation along SWs with different diameters, the dispersion curves for both symmetric and asymmetric modes are presented. Comparing with those given in previous literatures, in our results, the highest frequency is low and the frequency bands are narrow for all modes. The corresponding field patterns are obtained by simulations.

(ii) Based on the MDM of the Sommerfeld theory, the detailed physical analysis of the mechanisms for the radiative mode, the negative dispersion and the cutoff frequencies are presented.

(iii) Some physical phenomena, such as mode transformation, lifetime, resonance (asymptotic) frequency ω_s, are revealed and their mechanisms are explored.

As a simple and typical SPP transmission line, the results given in the paper will facilitate a general understanding of the features and the physics of the SPPs, not only for SW itself but also for other kinds of SPP transmission lines.

Appendix A: Formulas for the calculation of radiation power

For the fields outside of the wire:

$$E_z^{II} = C\mathrm{H}_m^{(1)}(k_c r)\mathrm{e}^{-\mathrm{j}\,k_z z}, \tag{A1}$$

$$\mathrm{H}_z^{II} = D\mathrm{H}_m^{(1)}(k_c r)\mathrm{e}^{-\mathrm{j}\,k_z z}, \tag{A2}$$

the radial Pointin vector per unite length can be obtained as

$$\begin{aligned} P_r &= \frac{1}{2}\,\mathrm{Re}\left\{\int (E_\theta^{II}\mathrm{H}_z^{II} - E_z^{II}\mathrm{H}_\theta^{II}) r\mathrm{d}\theta\right\} \\ &= -\frac{1}{2}\frac{\mathrm{j}\,\omega}{k_c^2}(\mu D^2 + C^2\varepsilon) \\ &\quad \times \mathrm{Re}\left\{\int (E_\theta^{II}\mathrm{H}_z^{II} - E_z^{II}\mathrm{H}_\theta^{II}) r\mathrm{d}\theta\right\} \\ &= \frac{2\omega}{k_c^2}(\mu\,|D|^2 + |C|^2\,\varepsilon), \end{aligned} \tag{A3}$$

where C and D are the constants relating to the excitation source, which can be determined by boundary

matching approaches, ω and k_c can be deduced from the dispersion relations.

According to the expression of the radial Poynting vector, when $k_c^2 = k_0^2 - k_z^2 > 0$, we can obtain $P_r > 0$, which means that there exists radiation in the radial direction.

Appendix B: Numerical calculation of resonance (asymptotic) frequency

With $v_g = 0$, the values of the resonance frequency ω_s for SPP propagation along the silver SW are numerically calculated here according to the dispersion equation (1), the calculation results of ω_s are listed in Table B1 with $K = k_z/k_p = k_z c/\omega_p$. Obviously, we can obtain a common value of $\omega_s = 0.3162$ rad/s for different diameters and mode numbers of SW, this value is the same as that obtained by Eq. (6) for the silver planar structure. The variation of the value of K with diameter of wire is shown in Fig. B1, indicating the process of frequency approaching to ω_s: the thinner the wire, the larger the value of K is, and the result is consistent with the dispersion behaviour of SW as shown in Fig. 3.

Table B1. Resonance (asymptotic) frequency for silver cylindrical structure.

ω_s	$n = 1$	$n = 5$	$n = 10$	$n = 15$	$n = 20$	$n = 30$
$D = 440$ nm	0.3162	0.3162	0.3162	0.3162	0.3162	0.3162
	($K \sim 20$)					
$D = 2004$ nm	0.3162	0.3162	0.3162	0.3162	0.3162	0.3162
	($K \sim 60$)					
$D = 100$ nm	0.3162	0.3162	0.3162	0.3162	0.3162	0.3162
	($K \sim 150$)					
$D = 44$ nm	0.3162	0.3162	0.3162	0.3162	0.3162	0.3162
	($K \sim 400$)					
$D = 10$ nm	0.3162	0.3162	0.3162	0.3162	0.3162	0.3162
	($K \sim 1400$)					
$D = 4.4$ nm	0.3162	0.3162	0.3162	0.3162	0.3162	0.3162
	($K \sim 2000$)					
$D = 2$ nm	0.3162	0.3162	0.3162	0.3162	0.3162	0.3162
	($K \sim 5000$)					

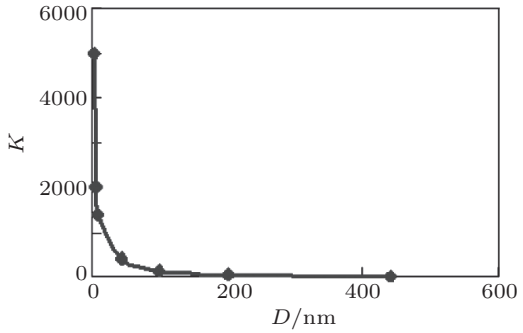


Fig. B1. Dependence of K on diameter of wire for the process of ω approaching to ω_s.

Thus, we can obtain the following results for ω_s:

i) from the view point of physics and optics, it represents that there is neither a signal nor energy transmission along the SW when the dispersion curves approach the line of ω_s and the resonance happens, the group velocity approaches to zero;

ii) the values of ω_s are the same for a planar and cylindrical structure;

iii) for a cylindrical structure, the value of ω_s is independent of wire diameter.

A similar situation happens to Au wire.

References

[1] Wang K L and Mittleman D M 2004 *Nature* **432** 376
[2] Cao Q and Jahns J 2005 *Opt. Exp.* **13** 18
[3] Wang K and Mittleman D M 2006 *Phys. Rev. Lett.* **96** 157401
[4] Pfeiffer C A, Economou E N and Ngai K L 1974 *Phys. Rev.* B **10** 3038
[5] Valk N C J van der and Planken P C M 2005 *Appl. Phys. Lett.* **87** 071106
[6] Wächter M, Nagel M and Kurz H 2005 *Opt. Exp.* **13** 10815
[7] Yang P F, Gu Y and Gong Q H 2008 *Chin. Phys.* B **17** 3880
[8] Wang J Q, Liang H M, Fang L, Li M, Niu X Y and Du J L 2009 *Chin. Phys.* B **18** 4870

[9] Monacelli B and Boreman G 2003 *Phys. Rev.* B **68** 155427
[10] Drude P 1900 *Zur Elektronentheorie der Metalle Annalen der Physik* **306** 566 (in German)
[11] Maier S A 2007 *Plasmonics: Fundamentals and Applications* (1st ed.) (Springer-Verlag)
[12] Ashcroft N W and Mermin N D 1976 *Solid State Physics* (Thomson Learning Asia Pte Ltd.)
[13] Johnson P B and Christy R W 1972 *Phys. Rev.* B **6** 4370
[14] Stratton J A 1941 *Electromagnetic Theory* (New York: McGraw-Hill)
[15] Schröter U and Dereux A 2001 *Phys. Rev.* B **64** 125420
[16] Stockman M I 2004 *Phys. Rev. Lett.* **93** 137404
[17] Reather H 1988 *Surface Plasmons on Smooth and Rough Surfaces and on Gratings* (New York: Springer-Verlag)